Evaluation of Analyses of Downstream Piping of Weirs by Model Experiments and Elasto-Plastic FEM

Kenji OKAJIMA [1] and Tadatsugu TANAKA [2]

[1]Assistant Professor, Graduate School of Agricultural and Life Sciences, University of Tokyo
(1-1-1, Yayoi, Bunkyo-ku, Tokyo, 113-8657, JAPAN)
E-mail: aokajim@mail.ecc.u-tokyo.ac.jp
[2] Professor, Graduate School of Agricultural and Life Sciences, University of Tokyo
(1-1-1, Yayoi, Bunkyo-ku, Tokyo, 113-8657, JAPAN)
E-mail: atanak@mail.ecc.u-tokyo.ac.jp

A creep flow theory, a critical velocity method and a critical hydraulic gradient method have been used as the safety criteria against seepage failure. These methods are reexamined by accurate model experiments and a numerical analysis. To develop the reliable method to evaluate seepage failure for foundation of a weir is important. A series of model experiments was performed and an elasto-plastic FEM was applied to the experiments. In the numerical analyses seepage force was put into the elasto-plastic FEM. The elasto-plastic FEM was shown to be valid method for the seepage failure problems. It was confirmed that the creep flow theory was not always effective as safeguard against seepage failure. Additionally it was suggested that Terzaghi's method was more effective than the creep theory to calculate the critical water head.

Key Words : *Seepage failure, Creep flow theory, Critical velocity method, Terzaghi method, Elasto-Plastic FEM*

1. INTRODUCTION

A creep flow theory is often applied to the design criteria against seepage failure. This theory was established as the empirical rules for the design of weirs on permeable strata through many experiences in 1910 (Bligh). After suggestion of this theory it was indicated that vertical sections of the creep line contribute more to reduce the danger of piping than horizontal sections of equal length. In the response to this, Lane (1935) suggested the weighted creep flow theory. These creep theories were based on the assumption that the cause of piping was erosion along the contact surface between soils and weir.

In addition, the critical velocity method and the critical hydraulic gradient method are applied to safety criteria against seepage failure. Justin method (1923), Koslova's method and Ohno's method (1984) are known as the critical velocity methods in Japan. The Terzaghi's method (1948) is famous as the critical hydraulic gradient. However these methods were formulated based on a one-dimensional theory and model tests. It was not evaluated intensively that these methods could be applied to safety criteria against piping of the weir foundation.

The purpose of this study is the reexamination of these practical safety criteria against seepage failure. We conducted a series of model experiments, and then evaluated these practical safety criteria and the validity of the elasto-plastic FEM by applying to the experiments.

2. A SERIES OF MODEL EXPERIMENTS

(1) Outline of model experiments

The experimental apparatus was consisted of a glass-walled sand box. The size of the box was 50.0cm×20.0cm×100.0cm (**Fig.1**). The permeable layers in these model experiments were made by using clean sand. The sand was the Toyoura sand

with a specific gravity of 2.64, a mean diameter (D50) of 0.16 mm and a uniformity coefficient of 1.46. The weir was made of rigid acrylic plates. The weir was fixed to sand box and was sealed by silicon rubber and silicon adhesion bond to prevent water and sand from spilling out. The wire gauze was pasted on the bottom of the weir to prevent roofing. The sand layers were prepared by pouring dry sand using hopper into stored water and deleting air during the soil particle falling. The high density of the sand layers was obtained: the relative density was 75～92%.

After setting up the water levels of both up-stream and down-stream side equal, the down-stream water level was lowered incrementally (5mm after an hour). The deformation of the sand layer was measured. When the soil layer was heaved about 1 mm, the water head was considered to attain the critical.

The data of a series of model experiments are indicated in **Table1**. These data were obtained by conducting 3 times in each experiment. These experiments are divided into 2 groups. The first group is the same penetration depth: Weir1, Weir2, Weir4 and Weir5. From these experiments we can evaluate the influence of the width of the weir for piping. The second group is the same creep length: Weir3, Wei4 and Weir6. From these we can evaluate the influence of Bligh's creep length.

(2) Results of model experiments

The critical head, flow, surface displacements of the sand layer were measured and the pictures were also recorded. A measuring point of the surface displacement using a laser displacement gauge was at a point which was located the center section of the sand box and 4cm down-stream from the weir.

The relationships between the water head and flow rate for experiments of Weir1, Weir2, Weir3 and Weir5 were indicated in **Fig.2**. Critical heads of all experiments were indicated in **Table2**. It was confirmed that from **Table2** critical heads of each experiments were almost coincident, and from Fig.2 the linearity of the relation of head to flow rate was hold until the critical head was attained.

Table 1. Designed data of a series of model experiments

Number of experiment	Width of the cistern	Penetration depth	Thickness of the sand layer	Creep length of Bligh
Weir 1	1cm	5cm	15cm	11cm
Weir 2	2cm	5cm	15cm	12cm
Weir 3	2cm	6cm	16cm	14cm
Weir 4	4cm	5cm	15cm	14cm
Weir 5	8cm	5cm	15cm	18cm
Weir 6	12cm	1cm	11cm	14cm

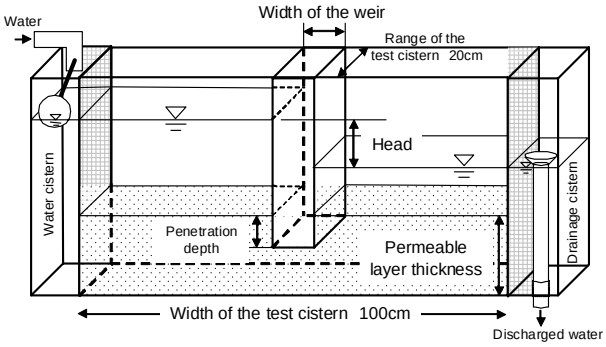

Fig.1 The concept and some sizes of the test apparatus

Table 2. Results of a series of model experiments

Number of experiment	Width of the cistern		Penetration depth	Creep length of Bligh	Reative density	The critical head
Weir 1	1cm	1st.	5.1cm	11.2cm	90.7%	18.0cm
		2nd.	5.0cm	11.0cm	80.7%	18.0cm
		3rd.	5.0cm	11.0cm	84.1%	17.0cm
Weir 2	2cm	1st.	5.0cm	12.0cm	87.6%	20.0cm
		2nd.	5.0cm	12.0cm	90.5%	19.0cm
		3rd.	5.1cm	12.2cm	84.6%	19.5cm
Weir 3	2cm	1st.	6.0cm	14.0cm	86.0%	23.0cm
		2nd.	6.2cm	14.4cm	92.1%	23.5cm
		3rd.	6.1cm	14.2cm	82.9%	23.7cm
Weir 4	4cm	1st.	5.0cm	14.0cm	76.9%	21.0cm
		2nd.	5.5cm	15.0cm	86.6%	22.0cm
		3rd.	5.1cm	14.2cm	87.9%	21.0cm
Weir 5	8cm	1st.	4.9cm	17.8cm	88.9%	26.5cm
		2nd.	5.0cm	18.0cm	85.1%	27.5cm
		3rd.	5.0cm	18.0cm	81.4%	27.5cm
Weir 6	12cm	1st.	1.0cm	14.0cm	89.4%	5.5cm
		2nd.	1.1cm	14.2cm	90.9%	6cm
		3rd.	1.0cm	14.0cm	92.0%	6cm

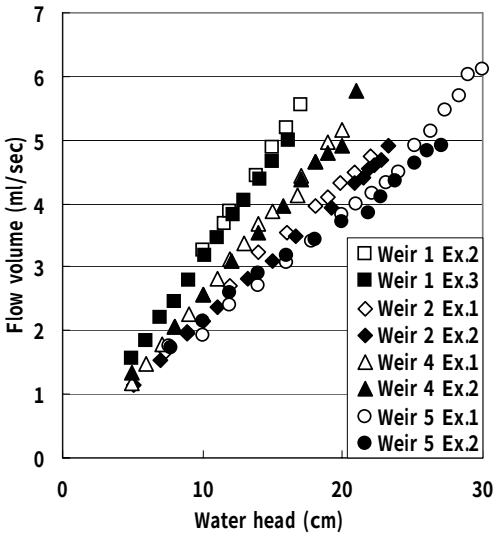

Fig.2 The relationship of water head to flow in Weir1, Weir2, Weir4 and Weir5

3. PRACTICAL DESIGN CRITRIA

(1) The creep flow theory

To prevent piping at the down-stream side of a weir, practical manuals indicate that a safe creep length have to be ensured under the surface of the weir and along the side of the weir. The creep length to be ensured must be larger than the values calculated by

two methods.

The first method is Bligh's method.

$$L_B \geq C_B \Delta H \tag{1}$$

Where L_B is the creep length that is measured along the bottom face of the weir, C_B is Bligh's creep ratio which varies depending on the type of the foundation soil, and ΔH is head of water. For example the fine sand C_B is 15. The critical head is ΔH_{CB} when $L_B = C_B \Delta H_{CB}$.

The second method is Lane's method.

$$L_L \geq C_L \Delta H \tag{2}$$

Where L_L is the weighted creep length.

$$L_L = \sum l_v + 1/3 \sum l_h \tag{3}$$

Where, l_v is the creep length of vertical direction (inclination angle of more than 45 degrees), l_v is the creep length of horizontal direction (inclination angle of lower than 45 degrees) and C_L is Lane's creep ratio which varies depending on the type of the foundation soils. For example the fine sand C_L is 7.0. ΔH is the water head. The critical head is , when $L_L = C_L \Delta H_{CL}$.

(2) The critical velocity methods

Justin (1923) proposed critical velocity that a soil particle started to move when the total stress P acting to the soil particle is equal to the submerged unit weight γ'.

$$V_c^j = \sqrt{\frac{\gamma' g}{A \gamma_w}} = \sqrt{\frac{2}{3}(G-1)dg} \tag{4}$$

Where V_c^j is Justin's critical velocity, A is the cross section of supposed flow tube, g is the gravitational acceleration, γ_w is the water unit weight, d is the particle size that impacts mainly on permeability, G is the specific gravity of the soil. Justin however, recommended that V_c^j is 0.25 (cm/sec) independent of the soil particle size.

Koslova and Ohno et al. proposed critical velocities based on each experiment. Koslova proposed critical velocity V_c^k from model tests with well graded soil.

$$V_c^k = 0.26 d^2 \left(1 + 1000 d^2 / {D_{50}}^2\right) \text{ (cm/sec)} \tag{5}$$

Where D_{50} is average soil particle size.

Ohno et al.(1984) proposed another critical velocity V_c^o from model tests with poor graded soil.

$$V_c^o = 10^{(1.95 \log d + 0.377)} \text{ (cm/sec)} \tag{6}$$

In Koslova's and Ohno's critical velocity D_{10} was applied to the particle size that impacts mainly on permeability; d. To apply these critical velocities to piping of foundation of weirs, in this study we combined the critical velocity with the analysis of seepage flow with FEM. We defined the critical head when the velocity of even one element in the soil layer finite element mesh exceeded the critical velocity.

(3) The critical hydraulic gradient

Terzaghi's method is the most famous method of a critical hydraulic gradient. Originally, Terzaghi's method was developed to be applied to a safety criterion for sheet pile piping. This method was formulated based on experimental model tests and its effectiveness was confirmed by many sheet pile model tests.

In Terzaghi's method, a piping occurs when the submerged weight of the soil prism on the down-stream side of the sheet pile equals the heaving force by excess hydrostatic pressure. In the formulation Terzaghi defined that the size of the prism was $D \times D/2$ in the two dimensional condition when the penetration depth is D.

$$\frac{1}{2} D \gamma_w h_a = \frac{1}{2} D^2 \gamma' \tag{7}$$

Where γ_w is the water unit weight. h_a is the average excess hydrostatic pressure acting to the bottom of prism.

4. SEEPAGE FAILURE ANALYSES BY ELASTO-PLASTIC FEM

In this study the finite element analysis consisted of two steps. The first step is the seepage flow analysis by FEM. The second is the seepage failure analysis by the elasto-plastic FEM with effective stress regarding the seepage force as the external force.

(1) Constitutive model of the elasto-plastic model

The finite element analysis employs the elasto-plastic constitutive equations with a non-associated flow rule and strain hardening-softening. The constitutive equations based on the yield function of Mohr-Coulomb and the plastic potential function of Drucker-Prager are applied. The finite element is 4-noded iso-parametric element with one point integration. In this analysis, the explicit dynamic relaxation method combined with the generalized return-mapping algorithm is applied. The elasto-plastic constitutive relations including the effect of the shear band are employed.

A simplified and generalized version of mesh size-dependent softening modulus method (Tanaka and Kawamoto, 1989) is used in this study. A material model for a real granular material (i.e., Toyoura sand) with a high angle of internal friction is used with the features of nonlinear pre-peak, pressure-sensitivity of the deformation and strength characteristics of sand, non-associated flow characteristics, post-peak strain softening, and strain-localization into a shear band with a specific width (Tatsuoka et al., 1991; Siddiquee, 1999). The material model will be briefly described in this section.

The yield function (f) and the plastic potential function (Φ) are given by

$$f = \alpha I_1 + \frac{\bar{\sigma}}{g(\theta_L)} = 0 \tag{8}$$

$$\Phi = \alpha' I_1 + \bar{\sigma} = 0 \tag{9}$$

where

$$\alpha = \frac{2\sin\phi}{\sqrt{3}(3-\sin\phi)} \tag{10}$$

$$\alpha' = \frac{2\sin\psi}{\sqrt{3}(3-\sin\psi)} \tag{11}$$

where I_1 is the first invariant (positive in tension) of deviatoric stresses and $\bar{\sigma}$ is the second invariant of deviatoric stress. With the Mohr-Coulomb model, $g(\theta_L)$ takes the following form.

$$g(\theta_L) = \frac{3-\sin\phi}{2\sqrt{3}\cos\theta_L - 2\sin\theta_L\sin\phi} \tag{12}$$

ϕ is the mobilized friction angle and θ_L is the Lode angle. The frictional hardening-softening functions expressed as follows are used.

hardening-regime:

$$\alpha(\kappa) = \left(\frac{2\sqrt{\kappa\varepsilon_f}}{\kappa+\varepsilon_f}\right)^m \alpha_p \qquad (\kappa \le \varepsilon_f) \tag{13}$$

softening-regime:

$$\alpha(\kappa) = \alpha_r + (\alpha_p - \alpha_r)\exp\left\{-\left(\frac{\kappa-\varepsilon_f}{\varepsilon_r}\right)^2\right\} \qquad (\kappa \ge \varepsilon_f) \tag{14}$$

where m, ε_f and ε_r are the material constants and α_p and α_r are the values of α at the peak and residual states. The residual friction angle (ϕ_r) and Poisson's ratio (ν) are chosen based on the data from the test of air-dried dense Toyoura sand. The elastic moduli are estimated using the following equations.

$$G = 900\frac{(2.17-e)^2}{1+e}\left(\frac{p}{p_a}\right)^{0.4} p_a \quad (p_a = 98kPa) \tag{15}$$

$$K = \frac{2(1+\nu)}{3(1-2\nu)}G \tag{16}$$

The peak friction angle (ϕ_p) is estimated from the following empirical relations based on the plane strain compression test on dense Toyoura sand.

$$\phi_p(\text{deg}) = \left\{59.47(1.5-e) - 10(1-e)\log\left\{\frac{\sigma_3}{(\sigma_3)_0}\right\}\right\} g_R(\delta) \tag{17}$$

$$(\sigma_3)_0 = 4(1-e)\,p_a \quad (p_a = 98kPa) \tag{18}$$

The peak friction angle is a function of confining pressure, initial void ratio e and angle δ of the direction of σ_1 relative to the horizontal bedding plane. The dilatancy angle (Ψ) is estimated from Rowe's stress-dilatancy relation.

The introduction of shear banding in the numerical analysis is achieved by introducing a strain localization parameter in the following additive decomposition of total strain increment as follows.

$$d\varepsilon_{ij} = d\varepsilon_{ij}^e + s\,d\varepsilon_{ij}^p \ , \quad s = F_b / F_e \tag{19}$$

where F_b is the area of a single shear band in each element; and F_e is the area of the element.

(2) Input parameters and FEM mesh

In the elasto-plastic finite element analysis, the material constants of Toyoura sand are as follow: relative density = 88%, residual friction angle (ϕ_r) = 33 degree. The calibration of the other elasto-plastic parameter of air-dried Toyoura sand in the elasto-plastic constitutive model was performed using the plane strain compression tests by Tatsuoka et al (1986). m= 0.3, ε_f = 0.1, ε_r = 0.6 and shear band thickness is 0.3 cm. The analysis was performed using a series of finite element mesh of each model

experiment, as shown in **Fig.3**. Elements bordering on the weir (elements colored gray in Fig.3) were boundary elements and in these elements the friction was set to be equal to the friction between sand and weir: a rigid and smooth surface. So the friction angle of the boundary elements was different from sand elements and was set to 12 degree. This friction angle was estimated from the study of Tatsuoka (1985).

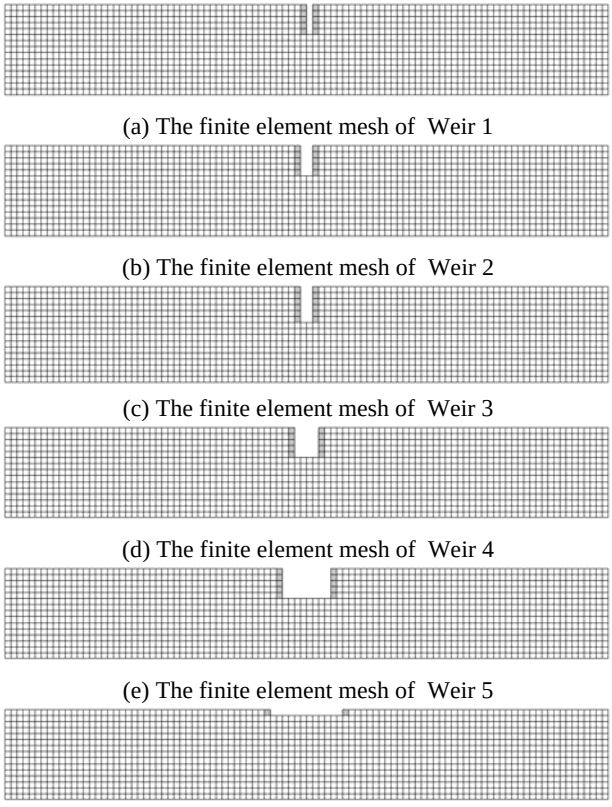

(a) The finite element mesh of Weir 1

(b) The finite element mesh of Weir 2

(c) The finite element mesh of Weir 3

(d) The finite element mesh of Weir 4

(e) The finite element mesh of Weir 5

(f) The finite element mesh of Weir 6

Fig.3 Finite element meshes for the seepage failure analysis

5. RESULT AND DISCUSSION

(1) Evaluation of the validity of elasto-plastic FEM

The relationships between critical water head and width of the weir in model experiments and elasto-plastic FEM of 1st group are indicated in **Fig.4**. From **Fig.4** the elasto-plastic FEM is able to express the critical head. However, the value of the FEM is a little lower than that of experiment. We need to taken into account that the results of experiments were affected by the boundary friction between soil layer and glass wall of sand box.

The picture of a seepage failure experiment at water head 27cm and the displacement of the FEM mesh at water head 23cm in Weir 5 were indicated in **Fig.5**. This picture and the displacement by the FEM had same displacement (about 0.45cm) at a measuring point (arrow). From **Fig.5** it was confirmed that the FEM was able to express the deformation of the soil layer just after critical head. The FEM was shown to be an effective numerical method of the seepage failure.

The contour line of the maximum shear strain at water head 23cm by the FEM of Weir 5 was indicated in **Fig.6**. The concentrated zone of shear strain appeared around down-stream of the weir was similar to a shape like prism.

(2) Evaluation of the creep flow theory

The creep ratio is considered to be safety factor in the creep flow theory. The creep flow theory by applying creep ratio gave too low critical head. So in this study we obtained the critical head without the creep ratio for the comparison between the creep flow theory and experiments.

The relationship between the critical head and the width of the weir in the same penetration depth (1st group) was indicated in **Fig.7**. From **Fig.7** results of the experimental series of the same penetration depth were that critical heads were increasing as the width of the weir became wider. Bligh's critical head was able to express this tendency well. But as the width of the weir increased, Lane's critical head was not able to express this tendency well.

The relationship between critical head and width of weir for the same Bligh's creep length (2nd group) was indicated in **Fig.8**. From **Fig.8** experimental critical heads for the same Bligh's creep lengths were decreasing as the width of the weir became wider. Results of experiments indicated that vertical sections of the creep length contribute more to reducing the danger of piping than horizontal length. Lane's critical head was able to capture this tendency, but Bligh's critical head was not able to express.

Bligh's creep theory and Lane's creep theory were not ineffective for the safety criteria against seepage failure. However it was apparent that these theories were not applicable to all cases of these experiments.

Variations of critical head with width of weir by elasto-plastic FEM were indicated in **Fig.7** and **Fig.8**. It was observed that the FEM was able to express the relationship between critical head and width of weir. The FEM of Weir 6 (the width was 12cm and the penetration depth was 1cm) predicted the critical head as rather danger side comparing to experiments. We thought the FEM mesh used was a little rough and the analysis should be carried out by more detailed mesh.

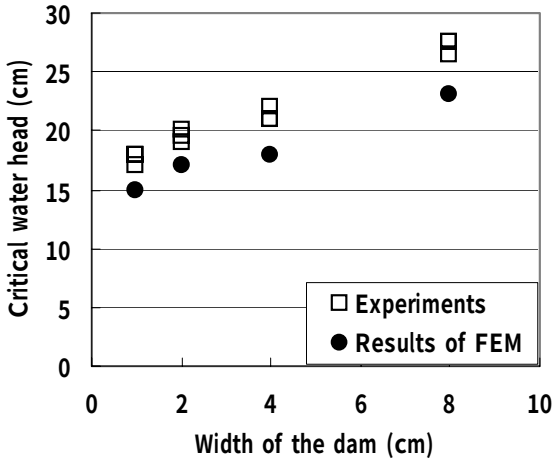

Fig.4 Relationship of critical water head and width of the weir

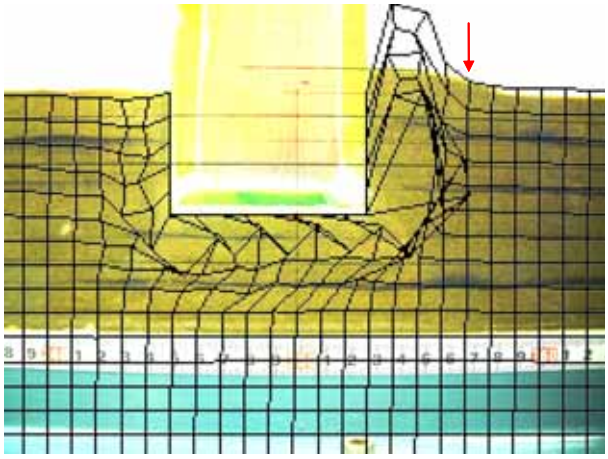

Fig.5 The picture of a seepage failure experiment at water head 27cm and the displacement of the FEM mesh at water head 23cm in Weir 5

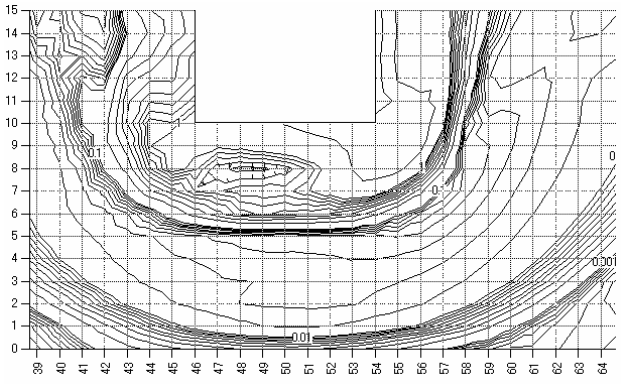

Fig.6 The counter line of the maximum shear strain distribution at water head 23cm in the FEM in Weir 5

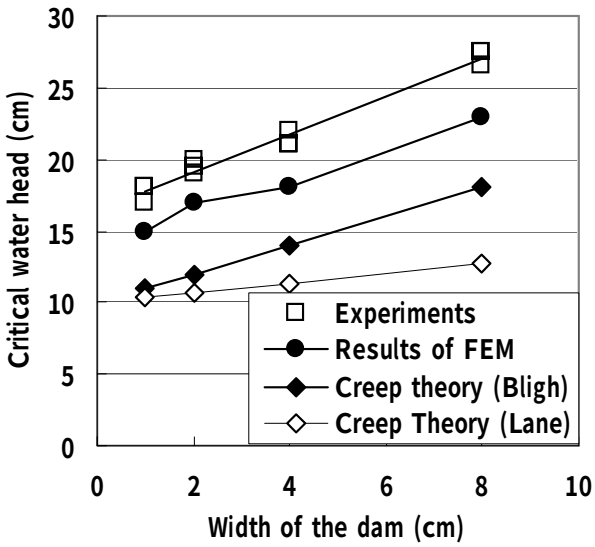

Fig.7 Relationship of critical head and the width of the weir in same penetration depth

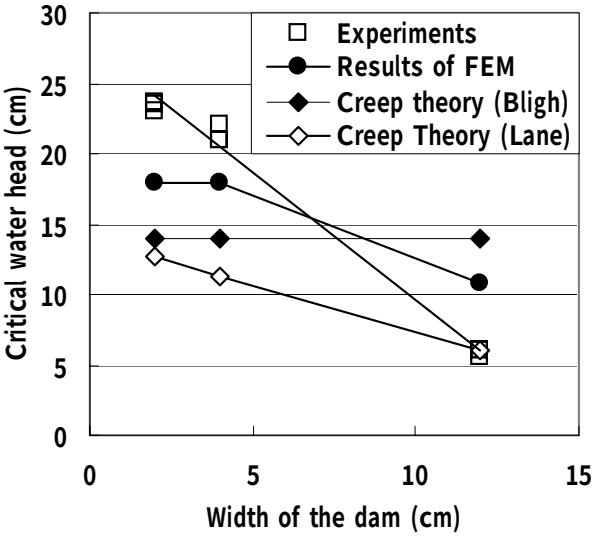

Fig.8 Relationship of critical head and width of the weir in same Bligh's creep length

(3) Evaluation of the critical velocity method and the critical hydraulic gradient method

The relationship between the effective particle size and the critical pore water velocity was indicated in **Fig.9**. We regarded 10% particle size as the effective particle size to seepage failure. 10% particle size of Toyoura sand is about 0.15mm. From **Fig.9** Justin's critical pore water velocity was about 2cm/sec. This velocity was too high for the estimation of seepage failure. Koslova's critical velocity was calculated with and this value for Toyoura sand is about 0.75. From **Fig.9** Koslova's critical pore water velocity was about 5cm/sec. This velocity was also too high for the estimation of seepage failure. The Koslova's critical velocity

method for the calculation of critical head was not applicable to the case of poor graded sand. In this study, modified Justin's critical velocity method and Ohno's critical velocity method were applied to the comparison between the critical head of critical velocity methods and experiments. Modified Justin's critical velocity was 0.25 (cm/sec) independent of soil particle size.

The relationship between critical water head and width of the weir for the same penetration depth (5cm) by the critical velocity method and Terzaghi's method was shown in **Fig. 10**. The relationship between the critical water head and width of the weir by the critical velocity method and Terzaghi's method for the same creep length (14cm) was indicated in **Fig.11**. From **Fig.10** and **Fig.11**, modified Justin's critical velocity method predicted the critical head to safe side excessively. This method was considered to be not applicable to safety criterion. Ohno's critical velocity method predicted critical heads as well as Bligh's creep theory. On the other hand, Terzaghi's method predicted critical head very well. It was the reason why the concentrated zone of shear strain around downstream of the weir which has the shape like prism was computed by our FEM as shown in **Fig.6**. The assumption of Terzaghi's method was verified by elasto-plastic FEM theoretically. It was obvious that Terzaghi's method was effective to predict the critical head of the foundation of the weir.

6. CONCLUSION

In this study the seepage failure of the weir was reexamined by a series of accurate model experiments and the elasto-plastic FEM. From this study it was indicated that the FEM was valid in seepage failure analysis of the foundation of the weir. It was apparent that creep flow theory was not able to express the critical head well in all the cases of experiments. Concerning the critical velocity method, Justin's critical velocity method predicted the critical head to safe side excessively. Ohno's critical velocity method predicted critical heads as well as Bligh's creep flow theory. Concerning the critical hydraulic gradient, Terzaghi's method which is applied mainly to the sheet pile piping, predicted critical head very well. This method was also confirmed by the maximum shear strain contour line by the elasto-plastic FEM. When the creep flow theory, the critical velocity method and the critical hydraulic gradient method are applied to safety criteria, it should be recognized that they involve the enough safety factor.

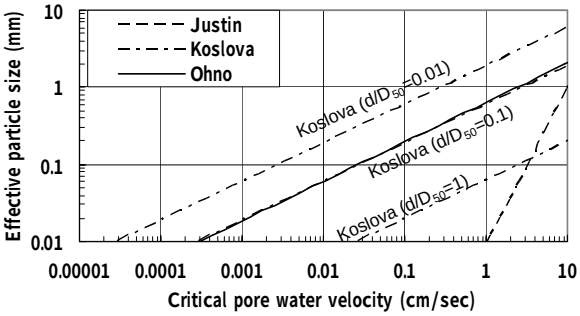

Fig.9 Relationship of the effective particle size and the critical pore water velocity

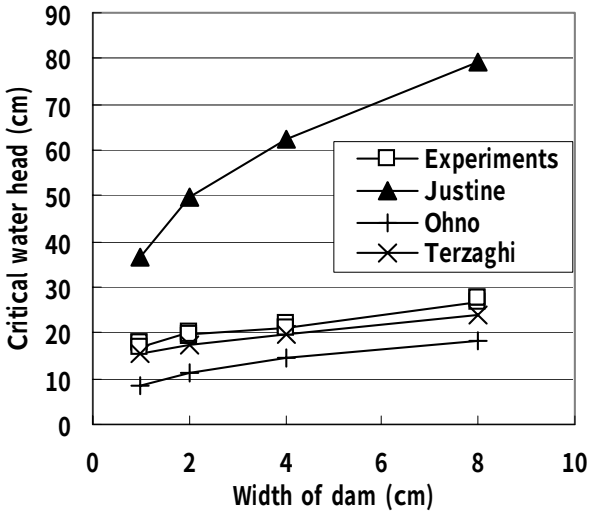

Fig.10 Relationship of critical water head and width of the weir in same penetration depth(5cm) by critical velocity method and Terzaghi method

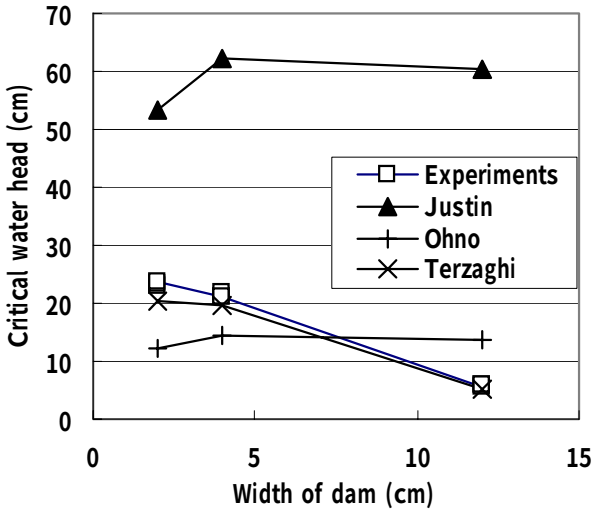

Fig.11 Relationship of critical water head and width of the weir in same creep length(14cm) by critical velocity method and Terzaghi method

REFERENCES

1) W.G.Bligh: The practical design of irrigation works, London Constable, 1910
2) Japanese Geotechnical Society: Handbook of Geotechnic, pp.1038-1043, 1999
3) J.D. Justin: The Design of Earth Dams, Trans. ASCE 87, pp.1-61, 1923
4) E.W. Lane: Security from Under seepage Masonry Dams on Earth Foundations, *Trans. ASCE*, 100, 1234-1351, 1935
5) Tsutomu Tanaka and Arnold Verruijt : Seepage failure of sand behind sheet piles – The mechanism and practical approach to analyze -, *Soils and Foundations* Vol.39, No.3, pp.27-35, 1999
6) Tanaka, T. and Kawamoto, O. : Three dimensional finite element collapse analysis for foundations and slopes using dynamic relaxation, *Proc. of Numer. Meth. in Geomech.*, Insbruch, 1213-1218, 1988
7) Tsutomu Tanaka and Arnold Verruijt : Seepage failure of sand behind sheet piles – The mechanism and practical approach to analyze -, *Soils and Foundations* Vol.39, No.3, pp.27-35, 1999
8) Fumio Tatsuoka and Osamu Haibara : Shear resistance between sand and smooth or lubricated surfaces, *Soils and Foundations* Vol.25, No.1, pp.89-98, 1985
9) Tatsuoka, F., Siddiquee, M. S. A, Park, C. S., Sakamoto, M. and Abe, F.: Modeling Stress-Strain Relations of Sand, *Soils and Foundations* Vol.33, No.2, pp.60-81, 1993
10) Karl Terzaghi and Ralph B. Peck : Soil Mechanics IN Engineering Practice, John Wiley and Sons, 1948